

## Research Paper

# How is urbanization shaping agricultural land-use? Unraveling the nexus between farmland abandonment and urbanization in China



Dawei Hou<sup>a,d</sup>, Fanhao Meng<sup>b,c,\*</sup>, Alexander V. Prishchepov<sup>d</sup>

<sup>a</sup> College of Public Administration, Nanjing Agricultural University, Nanjing 210095, China

<sup>b</sup> College of Geographical Science, Inner Mongolia Normal University, Hohhot 010022, China

<sup>c</sup> Inner Mongolia Key Laboratory of Remote Sensing and Geographic Information Systems, Inner Mongolia Normal University, Hohhot 010022, China

<sup>d</sup> Department of Geosciences and Natural Resource Management, University of Copenhagen, Copenhagen 1350, Denmark

## HIGHLIGHTS

- Farmland abandonment and recultivation due to urbanization was reconstructed with detailed time-series.
- Urbanization went hand-in-hand with farmland abandonment.
- Abandonment followed by a quick conversion to other land uses.
- Locational and socio-economic factors crucially determined farmland abandonment patterns.

## ARTICLE INFO

### Keywords:

Farmland abandonment  
Recultivation  
Urbanization  
Google Earth Engine  
Landsat imagery  
Logistic regression

## ABSTRACT

Urbanization often results in agricultural expansion but can also lead to farmland abandonment. However, it remains unclear about the extent, exact timing and determinants of farmland abandonment in response to ongoing urbanization. Using the example of China's Sunan economic region, we present the spatiotemporal trajectories of farmland abandonment and recultivation from 2001 to 2018. We classified Landsat satellite image time-series with a regression trees classifier in Google Earth Engine (GEE). Further, we analyzed the spatio-temporal patterns and rates of farmland abandonment and recultivation. Spatially-explicit logistic regressions were applied to explore the determinants of farmland abandonment in space and time. Our results show widespread farmland abandonment: approximately 232,700 ha of farmland had ever been abandoned from 2001 to 2018, with the highest annual abandonment rate (8.5%) in 2017. Approximately 66,200 ha of abandoned fields were later recultivated, with the maximum recultivated area (13,600 ha) in 2018. Approximately 92% of abandoned fields were later recultivated or reused as the impervious surface within two years of the first detection of abandonment, suggesting more rapid land transformation. The regressions reveal that locational and socio-economic factors determined farmland abandonment patterns. Specifically, a higher likelihood of farmland abandonment was statistically associated with an increased distance from the nearest settlements; the significantly positive relationship between 'Non-agricultural GDP' and farmland abandonment strengthened over time. In contrast, a lower likelihood of farmland abandonment was observed in areas with more cash crops. The statistical results may extend the application of the Ricardian comparative advantage theory along with Alonso's bid rent theory to explain and predict abandonment patterns in response to ongoing urbanization. Our study is the first attempt in China to apply 30-m Landsat imageries to reconstruct abandonment patterns over long time-series. The findings provide important insights into adjusting land-management practices for preventing farmland abandonment due to urbanization.

## 1. Introduction

Global societies are becoming increasingly urbanized, and this trend

is projected to continue in the future (Seto and Ramankutty, 2016). It is estimated that urbanized land will expand by another 1.2 million km<sup>2</sup> worldwide by 2030 (Seto et al., 2012). Urban land uses may compete for

\* Corresponding author.

E-mail address: [mfh320@imnu.edu.cn](mailto:mfh320@imnu.edu.cn) (F. Meng).

high-productive agricultural lands near settlements. However, urbanization may result in farmland contraction but also farmland abandonment (He et al., 2017). Farmland abandonment is a process when active fields cease to be cultivated, with or without vegetation recovery (FAO, 2006). Farmland abandonment has multiple implications for the environment and societal well-being (Baumann et al., 2011; Díaz et al., 2011). For instance, abandoned fields might serve as a source for wildfires (Dubinin et al., 2010). Abandoned fields may homogenize the traditional agricultural landscapes (Höchtl et al., 2005), yet foster improving hydrological regimes (Sileika et al., 2006). Farmland abandonment in the rural–urban context may significantly alter food security with local and distal implications regarding land use (Bren D Amour et al., 2017; Schierhorn et al., 2019; Seto et al., 2012).

Previous studies showed that abandonment rates and patterns differ substantially worldwide because various “exogenous” causes may alter agricultural land use. For instance, changing macroeconomic conditions (Kuemmerle et al., 2008; Lambin and Meyfroidt, 2010), agricultural production and demography changes (Prishchepov et al., 2012; Achieng et al., 2020), availability or the absence of agricultural subsidies (Milenov et al., 2014; Renwick et al., 2013) and rural–urban migration (Munroe et al., 2013), may trigger temporary or complete farmland abandonment (Prishchepov et al., 2021). Furthermore, predisposing “endogenous” site conditions, such as soil quality, precipitation and elevation, may foster or slow down abandonment processes following the causal “abandonment-driver” chain (Bürgi et al., 2004).

Among the proximate causes that trigger farmland abandonment, urbanization is of particular interest because it may go hand-in-hand with both economic development and the marginalization of neighboring areas (Elbakidze and Angelstam, 2007; Grădinaru et al., 2015). Urban sprawl may trigger the spread of impervious surface into highly productive farmlands near settlements with a long history of cultivation (He et al., 2017), while simultaneously lead to the abandonment in distant areas due to outmigration. For instance, urbanization had resulted in widespread abandonment on the Mediterranean coast and surrounding of European cities (Arnaez et al., 2011; Weissteiner et al., 2011). Despite a general expectation that more intensively cultivated areas can be found close to such settlements, the rural population exodus to urbanized areas may also lead to decreasing agricultural land-use intensity or even abandonment nearby the settlements (Grădinaru et al., 2015). Some farmlands nearby settlements can be temporarily abandoned, for instance, as a part of the legal conversion from farmland to the land designated for industrial or residential construction (Li et al., 2018; Liu et al., 2018). Similarly, the construction of buildings requires the preparation of construction sites on former farmlands. Therefore, this may result in the conversion of the agricultural plot to bare soil. However, depending on the success of the legal transformation of farmlands to urban and industrial use, the actual conversion of farmland may take years and sometimes decades, while the former agricultural fields may remain idle. In summary, farmland abandonment due to urbanization may present multiple land-use and land-cover trajectories in time and space.

There has been progress in studying the drivers of agricultural land abandonment in the last decades (Prishchepov et al., 2021). Yet, the understanding of how urbanization spatially and temporally determines farmland abandonment is patchy and cannot be easily transferred from one area to another. For instance, several studies demonstrated a higher concentration of farmland abandonment nearby cities as a precursor of built-up development (Grădinaru et al., 2015; Qiu et al., 2020; van der Zanden et al., 2017; Verburg and Overmars, 2009; Wang et al., 2020). As the urbanization process accelerates, people re-adapt urban space to maximize their profitability, and some economically more profitable

land uses may permeate into nearby agricultural areas. As a consequence, farmland near cities often becomes fragmented and less profitable for farming (Grădinaru et al., 2015). In contrast, some other studies found that remote agricultural plots that were farther from the urban fringe were more prone to be abandoned (Chaudhary et al., 2020; Meyfroidt et al., 2016; Vinogradovs et al., 2018; Zhang et al., 2014), resembling Von Thünen's location theory of land uses (Barlowe, 1986; Gellrich et al., 2007; Prishchepov et al., 2013). The increasing transportation costs and the lower demand for land rent, concomitant with low yields in distant places, may result in lower profit margins and further farmland abandonment (Zhang et al., 2014). In addition, urbanization could be characterized as an expansion of already existing urbanized areas or the conversion of rural settlements into urbanized centers, but it also involves the reallocation of labor resources between traditional farming and non-agricultural sectors of the economy. To some extent, Alonso's bid rent theory and Ricardian comparative advantage theory are also suited for explaining the trajectories of farmland abandonment due to urbanization, particularly with the decision of land-use agents to maximize their income. Hence, the nexus between abandonment and urbanization can be non-uniform in time and space and requires additional study.

Farmland abandonment is not a static but rather a transitional stage, resulting in multiple trajectories of an alternative to agricultural land uses (Prishchepov, 2020; Munroe et al., 2013). Furthermore, abandoned fields often emerge accompanying some other agricultural activities, such as fallows and crop rotation. Therefore, it is challenging to distinguish abandonment from transitional classes due to the complexity of the change process (Yin et al., 2018). Thirty-meter-resolution multispectral Landsat images are well suited for detecting land-use/land-cover change (LULCC), including farmland abandonment. The Landsat image archive provides high-resolution imagery with a long enough record to detect agricultural land-use trajectories in space and time (Dara et al., 2020). Recent work has also highlighted the potential of Landsat to map nuanced farmland abandonment. For instance, Dara et al. (2018) and Yin et al. (2020) developed new approaches to detect the extent and exact timing of farmland abandonment in the former Soviet Union with Landsat time series. Likewise, Landsat imagery proves to be a reliable source of data for mapping abandoned land in heterogeneous and highly fragmented urban settings (Grădinaru et al., 2019). Yet, to our knowledge, the application of Landsat imagery in identifying farmland abandonment is still restricted by the availability of cloud-free optical satellite imagery and the methodology allowing big data processing. In addition, no study has used the detailed Landsat time-series to map farmland abandonment in the region with the rapid urbanization of China.

The development of cloud-based processing of satellite imagery, such as Google Earth Engine, Sepal and AWS Amazon, has fundamentally changed the paradigm of satellite data access and processing (Gorelick et al., 2017; Zurqani et al., 2018). Google Earth Engine (GEE) is probably one of the most popular cloud platforms in the science community because it provides online open-access to Earth-observing remote sensing imagery, including USGS and ESA Sentinel products. Furthermore, GEE provides high-performance computing resources as well as state-of-the-art machine-learning algorithms that allow for the processing of satellite data (Patel et al., 2015). As it has significantly promoted the paradigm of data analysis and processing, GEE has been applied in multiple studies to investigate land-use/land-cover change (Ellison and Bachtrog, 2013; Li et al., 2015; Tsutsumida and Comber, 2015).

China represents an interesting case that allows us to reveal insights into the coupling between urbanization and farmland abandonment.

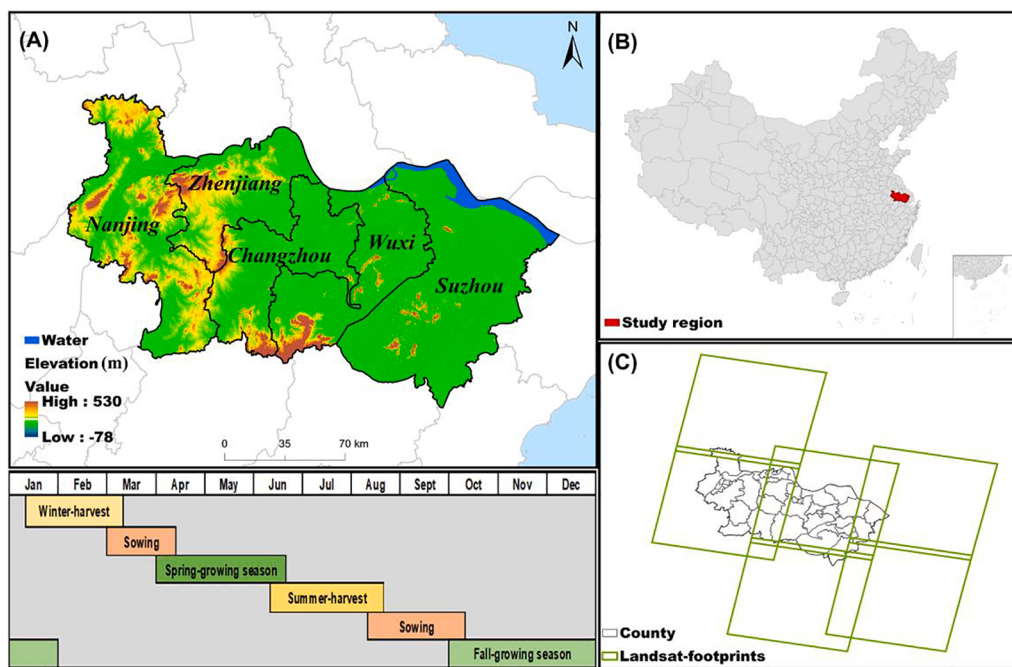


**Fig. 1.** Study region boundary and elevation (A). Location of the Sunan economic region in China (B). County boundary and Landsat-footprints (C) and Crop production cycle (bottom-left).

Since the implementation of the Open and Reform Policy in 1978, China has undergone drastic urbanization and socio-economic transitions (Liu et al., 2018), which have triggered widespread farmland abandonment (Deng et al., 2015; Seto and Kaufmann, 2003). Several studies have also shown farmland abandonment, including reforestation programs on former farmlands (Liu et al., 2020; Shi et al., 2018; Wang et al., 2020; Zhang et al., 2014). Among the hotspots of rapid socio-economic transition is the Sunan economic region, which is located in the lower reaches of the Yangtze River. Sunan has undergone urban sprawl and economic restructuring at an unprecedented rate since the mid-1980 s. Therefore, the region could serve as a ‘natural experiment’ to understand the shaping role of the ongoing urbanization in agricultural land-use patterns, including farmland abandonment. Additionally, the relative environmental homogeneity of Sunan can potentially reduce the impacts of environmental factors and thus enable a better focus on the contributions of the socio-economic transitions to abandonment patterns.

The overarching goal of our study was to advance the understanding of how ongoing urbanization could influence agricultural land-use. By using the example of China’s Sunan economic region, we mapped the spatiotemporal trajectories of farmland dynamics, including farmland abandonment and recultivation, from 2001 to 2018 with Landsat time-series and a classification and regression trees (CART) classifier in GEE. Further, we developed the spatially explicit logistic regression models at the pixel level for each year to explore the determinants of farmland abandonment. Our specific research questions were:

- 1) What are the inter-annual trajectories of land-use dynamic in the Sunan economic region of China from 2001 to 2018?
- 2) What are the extent and exact timing of farmland abandonment?
- 3) Which factors, triggered by urbanization, determine the spatial patterns of farmland abandonment?

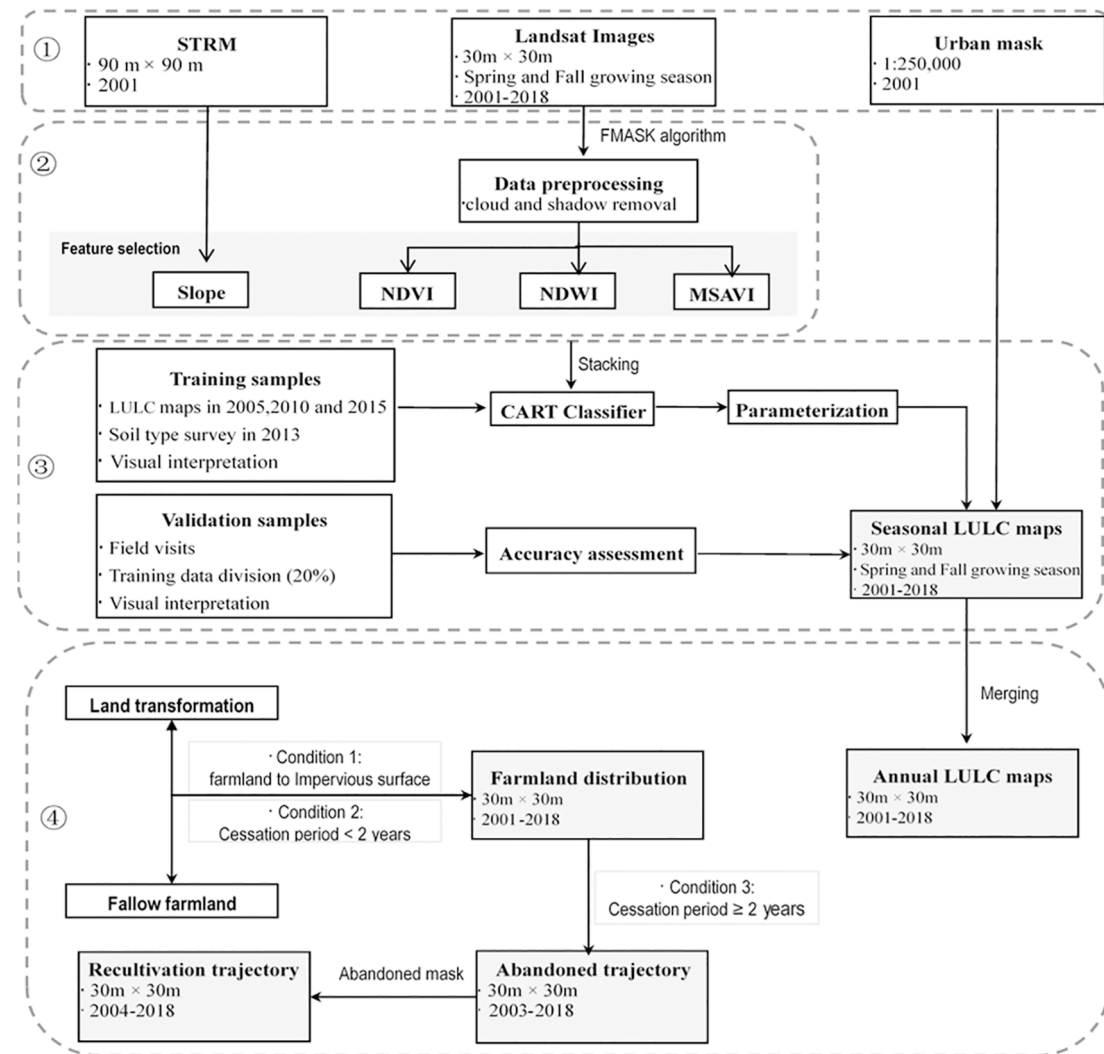
## 2. Methods

### 2.1. Study area

The study area is the Sunan economic region of China, which includes Nanjing, Zhenjiang, Wuxi, Changzhou and Suzhou municipalities. Sunan is situated at the lower reaches of the Yangtze River in the southern part of Jiangsu province (Fig. 1). The region covers approximately 27,945 km<sup>2</sup>, with an average elevation of 50 m. In 2017, Sunan had a population of 33.5 million, and the population density was 1,198 people/km<sup>2</sup>, which was eight times higher than the average population density in China (147 persons/km<sup>2</sup>). The average minimum temperature in the coldest month (January) varies from −7.4 to 3.7 °C, and the average maximum temperature in the warmest month (July) varies from 27.4 to 31.2 °C. The average annual precipitation amounts to 1,267 mm, and rainfall primarily occurs in January, December, June, July and August.

Sunan is well suited for agriculture, and two crop harvests per agricultural plot can be achieved annually. Specifically, the first crop-growing season (spring) usually lasts from early April to the middle of June, and harvest occurs from the end of June to the middle of August. The second crop-growing season (fall) usually lasts from the middle of October to the end of January, and harvest occurs from January to February (Fig. 1). The primary crops are wheat, barley, maize, silkworm peas, rice, soybean and potatoes. Historically, Sunan was regarded as one of the most important areas in China to provide agricultural commodities because of its superior productivity.

Since the implementation of the Reform and Opening-up Policy in 1978, Sunan has undergone rapid economic growth and drastic urban sprawl (Xie et al., 2007). By the end of 2018, the GDP per capita increased to approximately \$22,620, which was approximately 2.5 times higher than the average value (\$9,130) of China. Agricultural



Note: ① Data sources and inputs; ② Data preprocessing; ③ Sample selection and seasonal classification; ④ Mapping farmland abandonment and recultivation.

Fig. 2. Flowchart to summarize the process followed in this analysis.

sectors contributed only 1.7% to the total GDP, and the secondary and tertiary industries provided 40.55% and 56.05%, respectively. Furthermore, economic restructuring increased the share of off-farm employment from 75% in 2000 to 94% in 2018, while at the same time, urbanized areas expanded by approximately 4,000 km<sup>2</sup>.

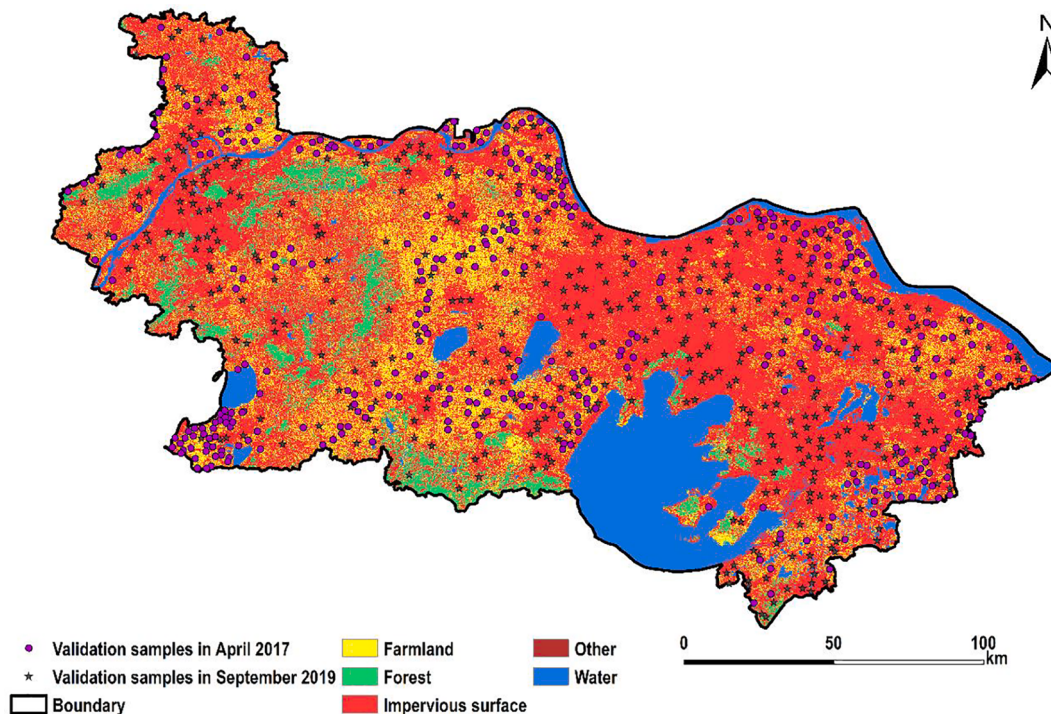
## 2.2. Acquisition of Landsat imagery and data preprocessing

To download, process and classify satellite imagery, we used the Google Earth Engine™ (GEE) service via the online platform and API Google Earth Engine™. To separately capture summer and winter crops, we acquired available Landsat imagery covering the spring-growing season (April 01-May 31) and fall-growing season (October 15–December 31) for all years between 2001 and 2018 from the Landsat archive available in GEE. In total, 216 Landsat surface reflectance images were acquired, and we used the Red, Green, Blue, NIR, SWIR 1 and SWIR 2 bands from Landsat 4, 5 TM, Landsat 7 ETM+ and Landsat 8 OLI imagery.

To minimize the impacts of clouds and shadows, we applied quality masks based on the FMASK algorithm (Zhu and Woodcock, 2012) to retain good-quality observations, for instance, by having satellite

imagery with less than 10% cloud coverage and retaining all available cloud-free pixels. Further, from the preprocessed Landsat surface reflectance products, we calculated three normalized indices for each Landsat image, which can highlight distinctive features of various land uses, namely, the normalized difference vegetation index (NDVI), normalized difference water index (NDWI) and modified soil adjusted vegetation index (MSAVI) (Gilabert et al., 2002; Huang et al., 2017; Jackson, 2004). The calculated indices were stacked into a multilayer image composite for subsequent classification (Fig. 2). We also felt that information about slope would help the classifier distinguish land-use and land-cover types in flatland and mountainous areas (Wright and Gallant, 2007). Therefore, we calculated the slope based on the STRM products and then added it into a multilayer image composite. To eliminate the misclassified farmlands within inner cities, we also digitized urban built-up areas for 2001 based on the regional land-use planning maps (1:250,000).

The classification catalog consisted of five classes: “farmland”, “forest”, “impervious surface”, “water” and “other”. Specifically, ‘farmland’ was defined as areas used for the production of grain crops or other cash crops during spring, fall or both seasons. ‘Impervious surface’ contained not only urbanized areas but also lands that have been



Note: we used the LULC maps in the fall growing season of 2018 as the background.

**Fig. 3.** Validation samples collected during the 2017 and 2019 field campaigns.

significantly modified by human activities in rural areas, such as rural residence and warehouse land. ‘Forest’ included deciduous, mixed forest, shrub and woody wetlands. ‘Other’ contained grassland, herbaceous wetlands, barren land (vegetation coverage <5%), rocks and sandy land.

### 2.3. Land-use and land-cover classification

A pixel-based, supervised classification and regression trees (CART) classifier was used to generate the maps of LULC classification. Classification and Regression Trees (CART) is a machine-learning method that allows land-cover categories to be classified by constructing prediction models from training data. CART can handle categorical binary features as well as continuous variables and is well suited to classify classes, such as agriculture, with a non-normal distribution of reflectance. CART is a prominent classifier for processing large datasets with high dimensionality (Johansen et al., 2015; Lozano et al., 2008; XU et al., 2005).

To parameterize CART, we prepared training data from three sources. The training data represented stratified random points, which were partially used for validation later. First, we used LULC maps at  $30 \times 30$  m resolution for 2005, 2010 and 2015. The maps were obtained from the Resource and Environment Data Cloud Platform (<http://www.resdc.cn/>). The three LULC maps were produced based on manual visual interpretation. The overall accuracy for these three maps was above 94.3%. A random sample of 1,000 points was made based on 2005, 2010, and 2015 LULC maps with a minimum distance of 500 m between points to reduce the potential spatial autocorrelation. Second, we prepared a set of training datasets from a soil-type survey in the fall of 2013. The training points were geolocated using a non-differential GPS and consisted of 723 sample points for ‘farmland’, 145 for ‘forest’, 257 for ‘impervious surface’, 185 for ‘other’ and 119 for ‘water’ classes. Third, for growing seasons in which we could not obtain training datasets from ready-to-use sources, training samples were created for each growing season by a visual interpretation of higher-resolution imagery (QuickBird and IKONOS) available via Google Earth™ mapping service. We created 150–1,000 training points per class depending on class

proportion for each growing season. These created training points were again selected with a minimum distance of 500 m to reduce the spatial autocorrelation. Finally, the training samples from the above three sources were uploaded into GEE for the classification (See the amounts of training samples for each growing season in Appendix Table A1).

We collected validation samples primarily from three sources to assess the classification accuracy, including the training data randomized division, field visits, and manual visual interpretation. Specifically, we first randomly selected 20% of the training samples per growing season as validation samples (Fig. 2). Second, we conducted two field visits in April 2017 and September 2019, respectively. We validated assigned land-cover classes during these visits and acquired the former classes and the exact land transition timing. We also interviewed the village leaders to assess the quality of the validation points. In total, we prepared 1,345 validation samples in the two field visits (Fig. 3), of which 542 sampled points represented LULC change classes. Third, another set of validation data was independently interpreted (no fewer than 50 points per class per growing season), and thematic classes were assigned based on visual interpretation of QuickBird and IKONOS images available at Google Earth. We calculated the confusion matrix, producer’s accuracy, user’s accuracy and overall accuracy for each classification to determine the applicability of our produced maps (See the amounts of validation samples for each growing season in Appendix Table A2).

### 2.4. Defining farmland abandonment and recultivation

We defined farmland abandonment as ‘farmland that had not been used for cultivation of crops in at least two consecutive years’. Recultivation was defined as ‘abandoned farmland that was cultivated again’.

Clean and green fallowing can be a part of crop rotation. To reduce the confusion between fallow and abandoned lands, we merged the LULC classifications of the two growing seasons for the same year. We labeled the pixel as ‘farmland’ if it was cultivated in either of the two growing seasons. We considered farmland to be abandoned if a pixel was

**Table 1**  
Explanatory variables.

Variable name	Time period	Source <sup>a</sup>	Spatial resolution
Distance to nearest settlement (km)	2001–2018	30 m Landsat TM/ETM + classifications	Pixel level calculations
Distance to nearest road network (km)		1:1000,000 road network maps	Pixel level calculations
*Non-agricultural GDP (10,000 CNY)		JSB	Rasterized county level statistics
Off-farm employment (10 <sup>4</sup> persons)		JSB	Rasterized county level statistics
Cultivated areas of cash crops (ha)		JSB	Rasterized county level statistics
Fertilizer inputs (ton)		JSB	Rasterized county level statistics
Agricultural machinery inputs (10 <sup>4</sup> kw)		JSB	Rasterized county level statistics
*Land prices (10 <sup>4</sup> CNY/ha)		CLT	Pixel level calculations
Agricultural suitability (dimensionless)		LMU/(Zabel et al., 2014)	Resampled 30arc seconds datasets

Note: <sup>a</sup>The following sources were used: JSB: the Statistical Bureau of Jiangsu Province; CLT: the website of China's land transaction ([www.landChina.com](http://www.landChina.com)); LMU: the Ludwig-Maximilians University. \* At 1978 constant prices.

**Table 2**  
Descriptive statistics for explanatory variables.

Variables	Level	Mean	St.d	Minimum	Maximum
Abandoned farmland	Pixel	0.102	0.302	0	1
Distance to the nearest settlement	Pixel	0.614	0.657	0.18	3.458
Distance to the nearest road	Pixel	0.209	0.203	0.085	1.283
Non-agricultural GDP	County	199.58	317.93	23.37	1881.91
Off-farm employment	County	39.89	14.36	3.7	78.98
Cultivated areas with cash crops	County	41.89	19.76	0.78	81.26
Fertilizer inputs	County	30,275	14,607	3697	46,506
Agricultural machinery inputs	County	37.45	13.41	4.73	65.5
Land prices	Pixel	996.91	804.04	10534.63	20424.58
Agricultural suitability	Pixel	0.646	0.235	0	0.92

identified as ‘farmland’ in the  $t$  th year and later identified as ‘other’ or ‘forest’ classes in the next two years ( $t+1$  and  $t+2$ ). We considered land to be transformed if the ‘farmland’ class transitioned to ‘impervious surface’. Finally, we summarized the spatial patterns of farmland abandonment from 2001 to 2018 to acquire the duration of abandonment. Similarly, we assessed and summarized the patterns and persistence of recultivation. For that purpose, we used the abandonment mask and traced whether the pixel was later converted to ‘farmland’.

To detect the spatiotemporal trajectories of farmland abandonment and recultivation, we calculated abandonment and recultivation rates. The abandonment rate was calculated according to the proportion of abandoned farmland relative to all farmland in the  $i$  th year, and the equation is as follows:

$$P_a = \frac{A_i}{TA_i} \times 100\% \quad (1)$$

where  $P_a$  represents the ‘abandonment rate’ in the  $i$  th year;  $A_i$  is the area of farmland abandonment in the  $i$  th year and  $TA_i$  represents the total area of farmland in the  $i$  th year.

The recultivation rate was calculated according to the percentage of abandoned farmland that was cultivated again (Yin et al., 2019), and the equation is as follows:

$$P_r = \frac{RA_{i+1}}{A_i} \times 100\% \quad (2)$$

where  $P_r$  is the ‘recultivation rate’ in the  $(i+1)$  th year and  $RA_{i+1}$  represents the area of recultivation in the  $(i+1)$  th year.

## 2.5. Explanatory variables

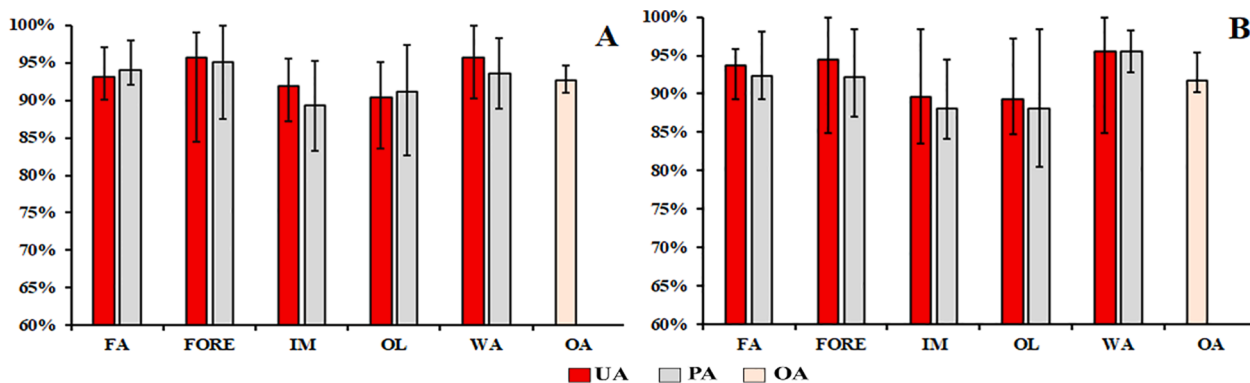
A rapid shift from an agricultural to an urbanized society often results in sharply urbanized land expansion but also changes in economic decisions and livelihood strategies (Han and Song, 2019). Therefore, we assumed that farmland abandonment was simultaneously driven by spatial reconfiguration of landscapes and economic decisions. Based on this assumption, we selected explanatory variables that may reflect the locational characteristics and market accessibility of agricultural practices, including the distance to settlements and the distance to roads (Table 1). Economic theory often portrayed farmers as rational agents who strive to shed excess labor by engaging in off-farm economies and readapting farming structures to maximize their income (Gellrich et al., 2007). We thus included non-agricultural Gross Domestic Product (GDP), the number of persons engaging in non-farming sectors and the cultivated areas of cash crops in this analysis. In the process of urbanization, peri-urban farmland owners may prefer temporary agricultural practices with lower investments to speculate on rising land prices due to the increasing demand for non-farming land for urban development (Zhou et al., 2020). Based on this assumption, we acquired annual land prices in the Sunan economic region to reflect the impacts of land speculation on farmland abandonment. Furthermore, we also assumed that the input intensity of agricultural plots crucially determines the decisions associated with agricultural practices, including abandonment. We thus selected the determinants representing the input intensity including fertilizer and agricultural mechanization in this analysis (Table 1).

The most detailed statistics for Sunan economic region were available at the county level, equivalent to the NUTS 4 or LAU 1 in the Nomenclature of Territorial Units for Statistics of the EU. The average size of counties in Sunan is 738 km<sup>2</sup>, and our statistical analysis covered 30 counties (6 in Changzhou, 7 of 11 in Nanjing, 5 of 9 in Suzhou, 6 in Wuxi and 6 in Zhenjiang) (see Table 2).

To evaluate the locational characteristics of abandoned fields, we developed a multi-centric urban model to acquire the spatiotemporal trajectories of urban sprawl (Kroll et al., 2012; Larondelle and Haase, 2013). For such calculation, we retained only settlements with a population larger than 500,000 people because we assumed that such settlements could provide enough off-farm employment and socio-economic services to attract rural dwellers. Subsequently, we calculated the Euclidean distance of abandoned fields to the annually updated urban fringe. Furthermore, as a measure of infrastructure and market accessibility, we calculated the distances of agricultural plots to the nearest road by using annually updated road network datasets (1:100,000) in the Sunan economic region (Table 1).

To capture the effects of ongoing urbanization on farmers’ economic decisions, we obtained county-level statistics by proxying socio-economic variables, including non-agricultural GDP, the number of persons engaging in non-farm sectors and the cultivated areas of cash crops. Specifically, the cash crops mainly included vegetables, fruits and tea. Furthermore, we acquired the county-level statistics including fertilizer inputs and agricultural mechanization inputs to proxy the variables on agricultural input intensity.

To measure land speculation effects due to ongoing urbanization, we acquired the annually point-level land prices datasets from [www.landChina.com](http://www.landChina.com). From 2001 to 2018, a total of 789 points were recorded in Sunan to represent every patch’s specific prices that sell out the agricultural plots to developers for non-farming uses. We annually digitized the land prices points and interpolated them using Kriging methods to obtain general distributions (Table 1).



Abbreviation: FA—‘farmland’; FORE—‘forest’; IM—‘impervious surface’; OL—‘other’; WA—‘water’; UA—‘User’s accuracy’; PA—‘Producer’s accuracy’; OA—‘Overall accuracy’. The values on the bar chart represent the median accuracy per class across all spring growing seasons (A) and all fall growing seasons (B), while the confidence intervals represent the accuracy-float range.

Fig. 4. The accuracy for 18 spring-growing seasons (A) and 18 fall-growing seasons (B).

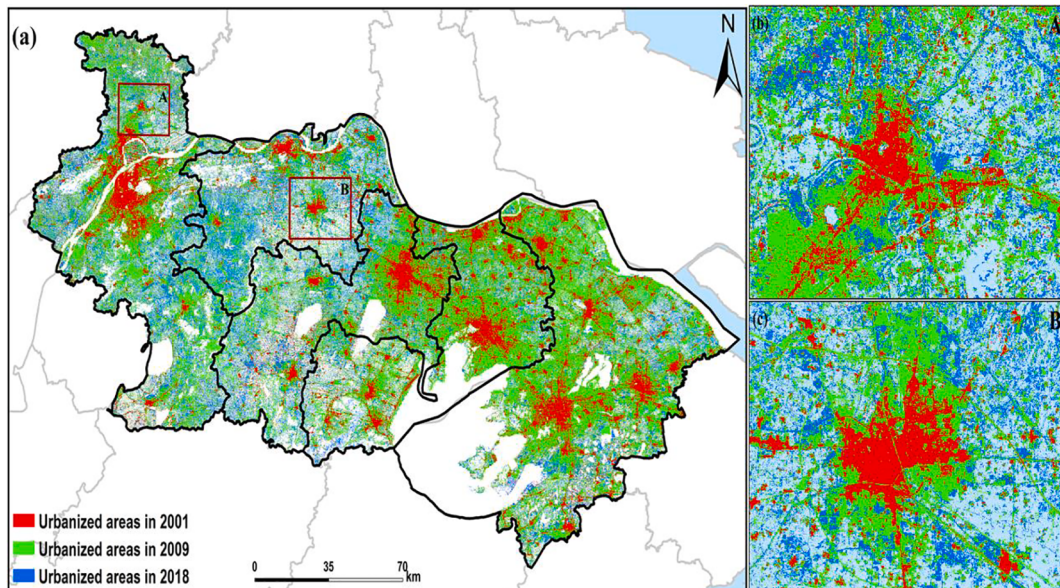


Fig. 5. The spatiotemporal trajectories of urban sprawl in China's Sunan economic region from 2001 to 2018.

To evaluate the impact of agricultural suitability on land-cover change patterns, we acquired the datasets of general agricultural suitability (2011–2040) from the Ludwig-Maximilians University (LMU). The map can be regarded as a comprehensive representation of natural suitability for cultivation because it was computed using a fuzzy logic approach according to the climatic, soil and topographic conditions at a spatial resolution of 30 arc seconds (Zabel et al., 2014).

All of the nine variables we selected were rasterized and resampled at 30-m resolution to match our produced LULC maps derived from the Landsat TM/ETM + satellite images.

## 2.6. Logistic regression

To evaluate the determinants of farmland abandonment, we developed spatially logistic regression models at the pixel level for each year. For the logistic regressions, we treated “farmland abandonment” as the dependent variable and used the nine variables we selected as independent variables (Table 1). We defined “1” as “abandoned farmland”

and “0” as “non-abandoned farmland”. Areas that were covered by other land-cover types were excluded from our analysis.

We first measured the spatial autocorrelation of abandoned fields with global Moran's I and then acquired samples covering the entire area. We maintained a gap of at least 300 m between samples to reduce Moran's I by 0.17–0.35. Multiple samples within the same administrative unit may not be absolutely independent (Gellrich et al., 2007; Müller and Munroe, 2008) because land-use decisions may systematically affect decision-making by local producers regarding agricultural land-use (Müller et al., 2014). For this reason, we introduced a statistically clustered adjustment and a Huber–White sandwich estimator to control the potential spatial autocorrelation by assessing robust standard errors without affecting the estimated coefficients in the model (Huber, 1967; White, 1982). We used StataSE 15 for above statistical analysis and assessed the goodness-of-fit of the logistic regressions for each year using the area under the ROC curve (AUC), the log-likelihood and Nagelkerke R<sup>2</sup>.

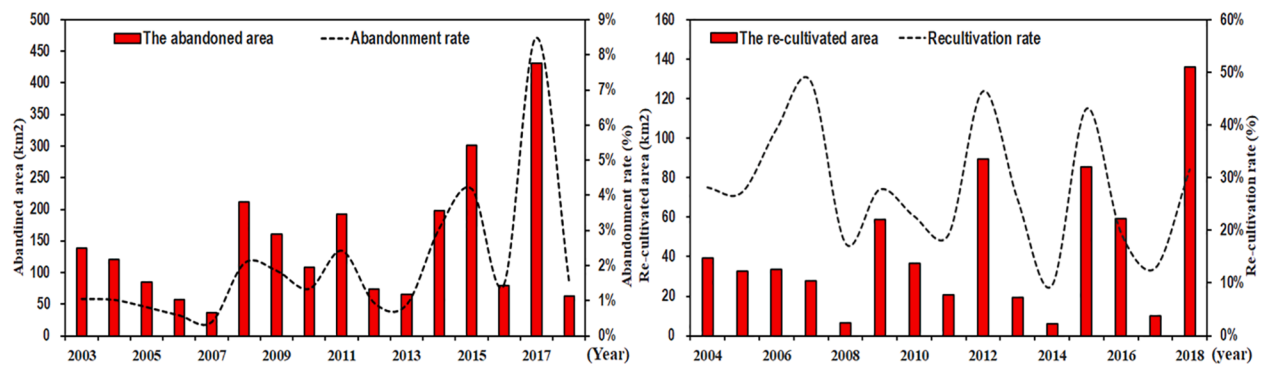


Fig. 6. The annual abandonment increment and abandonment rate (the left) and the annual recultivation increase and recultivation rate (the right).

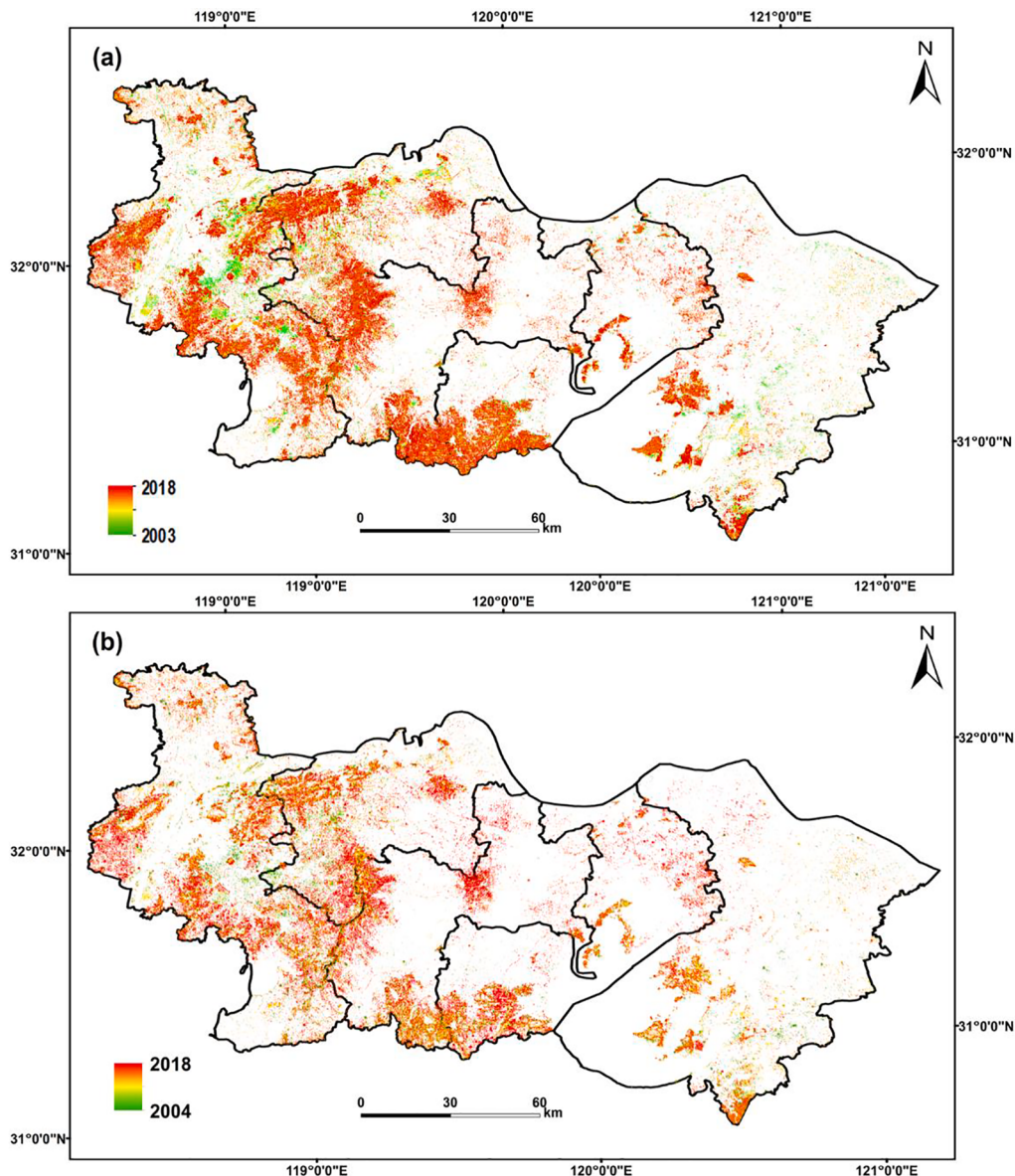
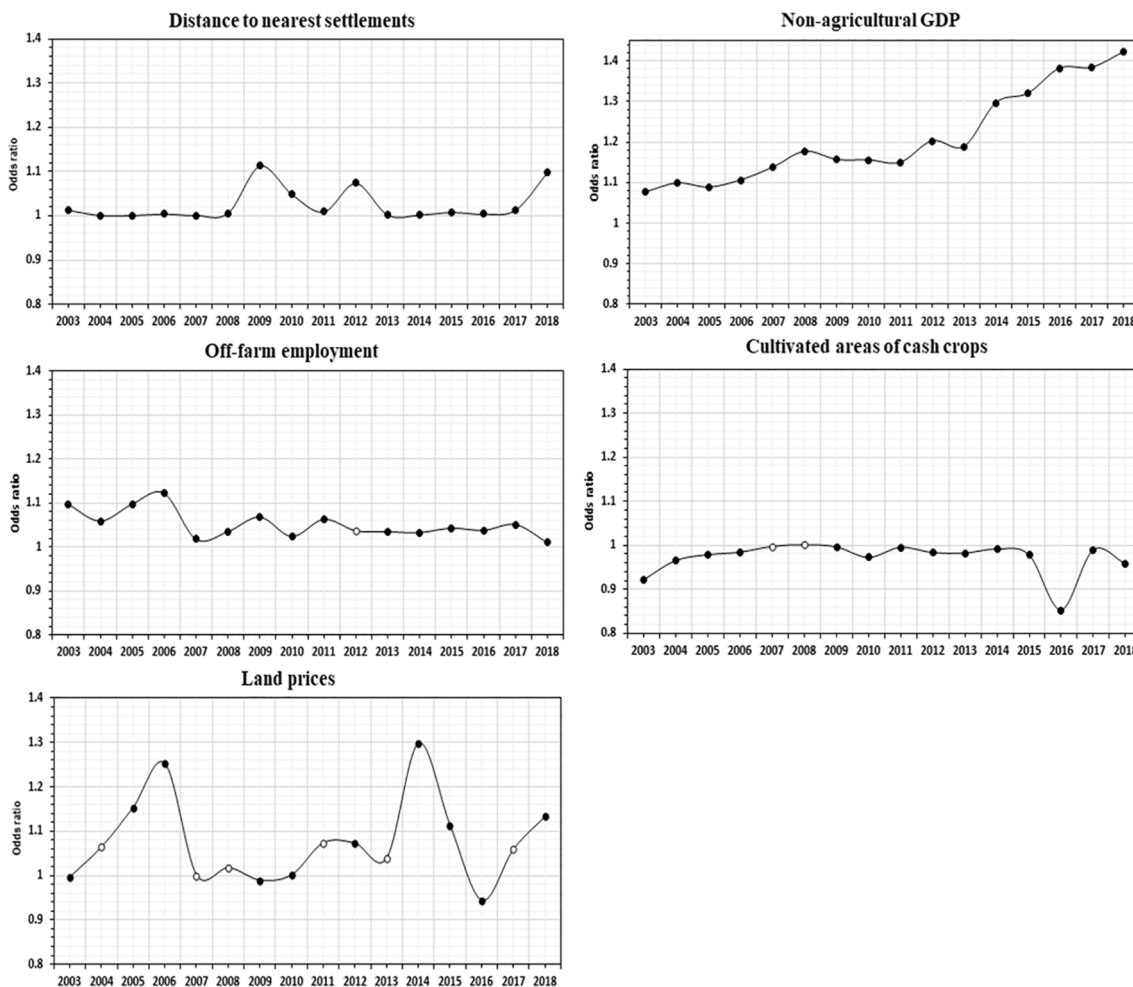


Fig. 7. Location and timing of abandonment (a) and recultivation (b) in the Sunan Economic Region.



Note: the filled black circles represented significant results in the models and the empty circles were the non-significant results.

Fig. 8. The tendency of the odds ratio of the five key variables in spatial logistic regression.

### 3. Results

#### 3.1. Classification accuracy and inter-annual land-use dynamic

We reconstructed land-cover dynamics across 36 growing seasons from 2001 to 2018 (18 spring- and 18 fall-growing seasons) with 30-m-resolution Landsat imageries and the CART method in GEE (Appendix Fig. A3 and Appendix Fig A4). The overall classification accuracy varied from 91.03% to 94.62% for the spring growing season and from 90.25% to 95.42% for the fall growing season, respectively. For the 'farmland' class, producer's accuracy varied from 89.26% (2009 fall growing season) to 98.16% (2016 fall growing season), and user's accuracy varied from 89.34% (2008 fall growing season) to 97.13% (2018 spring growing season). For 'water', producer's and user's accuracies were above 90%. For the 'forest' class, we reached the lowest (84.5%) and highest user's accuracy (99.1%) in the spring growing seasons of 2004 and 2010, respectively. As the fuzzy spectral signature between barren land and impervious surfaces, the lowest producer's and user's accuracies were obtained for 'impervious surface' and 'other' classes, but they were still above 80% (Fig. 4 and Appendix Table A5).

We produced annual land-cover maps from 2001 to 2018 by merging spring- and fall-season maps for each year. The temporal trajectories revealed that Sunan underwent drastic urban sprawl, shifting from an agriculture-dominated to a highly urbanized landscape (Fig. 5). The

share of 'impervious surface' increased from 12% in 2001 to 63% in 2018, equaling a total increase of  $1.53 \times 10^6$  ha. Furthermore, approximately 94% of new 'impervious surface' ( $1.434 \times 10^6$  ha) emerged at the expense of 'farmland', and only 30,800 ha and 29,900 ha emerged for 'forest' and 'other', respectively. A visual inspection of the produced LULCC maps revealed that the accelerated urban sprawl resulted in significant aggregation and connectivity of settlements, particularly in western parts. Specifically, 51 settlements with more than 500,000 people were identified in 2001, while the number decreased to 16 by the end of 2018. Furthermore, the total area of 'forest' and 'water' did not show a dramatic decrease and was relatively stable from 2001 to 2018. At the same time, the 'other' class, which included grasslands, underwent a drastic decrease, and only 3,600 ha remained.

#### 3.2. Spatiotemporal trajectory of farmland abandonment and recultivation

Our results showed that farmland abandonment was a widespread LULCC phenomenon throughout the Sunan economic region of China. Approximately 232,700 ha of actively cultivated farmland had ever been abandoned during the study period, equaling to 11.6% of farmland cultivated in 2001. Specifically, the maximum abandonment of 43,100 ha was observed in 2017, followed by 30,100 ha in 2015 and 21,200 ha

in 2008. We also noticed that there were marked differences in abandonment rates, with the highest abandonment rate of 8.5% and the lowest abandonment rate of 0.4% observed in 2017 and 2007, respectively (Fig. 6). Spatially, abandoned fields were not distributed uniformly across the whole area but were clustered in western and southern parts, whereas they were more dispersed in the plains of the eastern part of the Sunan economic region (Fig. 7a).

Out of 232,700 ha of abandoned farmland, approximately 72% (166,600 ha) transitioned to ‘impervious surface’ and ‘forest’ by 2018, whereas only 66,200 ha (about 28%) was recultivated. The recultivation did not show a significant temporal consistency compared with farmland abandonment. The greatest extent of recultivation was observed in 2018 when 13,600 ha of abandoned farmland was recultivated, whereas only 620 ha of abandoned farmland was recultivated in 2014. The highest recultivation rate of 48.3% occurred in 2007, and the lowest rate of 9.5% was in 2014 (Fig. 6). Recultivation was spatially concentrated in western and southern parts (Fig. 7b). Our findings also showed that all the abandoned fields were converted, for instance, to ‘impervious surface’ or were recultivated within a five-year period. More specifically, approximately 92% of abandoned farmland was recultivated or converted into ‘impervious surface’ within a two-year period of the first detection of abandonment.

### 3.3. Determinants of farmland abandonment

The Nagelkerke R<sup>2</sup>s of the logistic regressions for each year ranged from 0.153 to 0.69, indicating that the explanatory power of the logistic regression models fluctuated during our study period. We should interpret the measures with caution because the standards of the goodness-of-fit in conventional regression analysis may not be absolutely suitable to explain the results of spatial logistic regressions at the pixel level (Hosmer and Lemeshow, 2000; Gellrich et al., 2007; Müller and Munroe, 2008; Prishchepov et al., 2013). The area under the ROC curve (AUC) for all logistic regression models exceeded 0.88, indicating that at least 88% of pixels can be correctly distinguished between abandoned farmland and stable farmland, and the results were better than the likelihood that the two classes were separated stochastically (AUC = 0.5) (Please see the supplementary appendix).

The inter-annual logistic regression analysis shows that locational characteristics and socio-economic variables were the most important variables to explain farmland abandonment patterns associated with ongoing urbanization in the Sunan economic region of China, whereas some other variables covering input intensity and agro-environmental suitability of farmland showed weak correlations in space and time.

Among the proximity variables, ‘Distance to nearest settlement’ was significant and had a positive correlation with farmland abandonment for all 16 regression models. Furthermore, all of the odds ratio in the 16 regression models varied but were larger than 1, indicating that an increased distance from the nearest settlement would increase the likelihood of farmland abandonment. For instance, in 2012, the likelihood of observing abandoned plots increased by 7.4% for every 1 km of moving away from the urban fringe (odds ratio = 1.074) (Fig. 8).

‘Non-agricultural GDP’ was also positively significantly correlated with farmland abandonment across all the 16 regression models. The odds ratio of ‘Non-agricultural GDP’ presented an overall increasing tendency from 1.076 in 2003 to 1.421 in 2018, indicating that the impacts of the acceleration of non-agricultural sectors on agricultural land-use strengthened over time.

‘Off-farm employment’ was statistically significantly correlated with farmland abandonment in the 15 of 16 regression models. Similar to ‘Distance to nearest settlement’, the odds ratios of ‘Off-farm employment’ fluctuated but were larger than 1, indicating the positive correlations with farmland abandonment. For instance, an increase of 10,000 persons engaging in off-farm employment in 2018 would increase the likelihood of farmland abandonment by 1% (odds ratio = 1.010).

Farmland abandonment was significantly negatively correlated with

‘Cultivated areas of cash crops’ in 14 regression models, indicating that agricultural areas which were engaged in production of higher value crops had a lower likelihood of being abandoned compared to fields occupied by cereal crops. For instance, abandonment was 15% less probable at the county level for an increase of 1 ha of cultivating cash crops in 2016 (odds ratio = 0.852).

From 2003 to 2018, ‘Land prices’ presented unstable correlations with farmland abandonment in the Sunan economic region of China. Specifically, 10 of the 16 regression models showed a statistically significant relationship with farmland abandonment, whereas the other six statistical results were not significant. Furthermore, the odds ratio of ‘Land prices’ fluctuated around 1, indicating that the correlation fluctuated over time and the influences of land prices on farmland abandonment should be interpreted with more cautions by combining with some other exogenous causes, such as contemporary land-use policies.

## 4. Discussion

Our study revealed the spatiotemporal trajectories of farmland abandonment and recultivation in response to ongoing urbanization in the Sunan economic region. To our knowledge, this is the first attempt in China to employ the detailed Landsat time-series to reconstruct farmland abandonment due to ongoing urbanization. Our major contribution and improvement can be summarized in three aspects. First, GEE provided us an opportunity to collect all available images and automatically process satellite data in the cloud computing environment, thereby making it possible to analyze LULC with detailed time-series. Second, we analyzed two annual growing seasons separately, and this allowed us to minimize the impacts of the fuzzy spectral signature and the complexity of double cropping. At the same time, we also controlled for inter-annual fallow as a part of crop rotation. Third, we reconstructed the inter-annual patterns and moved away from temporally coarse land-change intervals, which have often been used in the past (Baumann et al., 2011; Kuemmerle et al., 2008; Prishchepov et al., 2012). Such spatially and temporally explicit maps allowed us to evaluate more nuanced relationships between determinants and farmland abandonment and to specify the reshaping role of urbanization in agricultural land-use changes in space and time.

Our satellite image analysis showed widespread farmland abandonment throughout the Sunan economic region. However, the extent and rate of abandonment differed greatly across the study years. In general, we observed a total of 11.6% farmland in Sunan had ever been abandoned, with an annual abandonment rate of 2%. The rates of abandonment were much lower than those reported in the mountainous areas of China, ranging from 14.32% to 27.2% (Han and Song, 2019; Wang et al., 2020). Compared to worldwide results, the abandoned rates were also lower than the outcomes in Eastern Europe and the former Soviet Union and Chile, ranging from 16% to 45% (Baumann et al., 2011; Díaz et al., 2011; Lieskovský et al., 2015; Prishchepov et al., 2012), but similar to Central Asia (13%) (Löw et al., 2018). Furthermore, Sunan had a shorter duration of abandonment before being recultivated or reused for non-agricultural uses, suggesting more rapid land transformation. This feature may be attributed to the increasing demands for urban sprawl in response to the rapid development of non-agricultural sectors. The Sunan economic region had used only 0.29% of China’s territory to generate about 6.4% GDP, which has become one of the most important economic-geographic units. However, with the rapid development of non-agricultural sectors, Sunan has attracted a large number of rural labor forces, which caused about 8.3 times population density higher than the average value of China. To match the increasing demands for infrastructure services, urban sprawl inevitably accelerated and even emerged at the expense of productive soils near cities (Ge et al., 2018; Xu et al., 2019).

Our modeling results suggest that within the Sunan economic region of China, the higher likelihood of farmland abandonment emerged in areas far from the urban fringe, in counties with higher contribution to

the economy from non-agricultural sectors, and in counties with more off-farm employment. One of the main lessons from the statistical analysis is that locational characteristics and socio-economic transitions crucially shaped the spatial pattern of agricultural land-use in rapidly urbanized areas. Agricultural plots had a higher likelihood of being abandoned if they were located farther from the urban fringe and food market. The statistical relationship between abandonment and urbanization appears to coincide with Von Thünen's theory that agricultural patterns are substantially determined by the increasing importance of locational characteristics and transportation costs. However, we suggest that Von Thünen's model should be used with caution because gaps in accessibility will be gradually filled in such urbanized areas. For instance, in the Sunan economic region, the total length of the road network (including major and secondary road) increased by 2.5 times from 19,910 km in 2001 to 46,967 km in 2018. Thus, the role of transportation costs in the determination of land use in Von Thünen's theory, with the improvement of the road network and better vehicles, may be overstated. Furthermore, we should also account for the strong roles of the government in the determination of land uses when rapid urbanization forces the government to allocate agricultural lands for further urban expansion.

The economic development from non-agricultural sectors strengthened farmland abandonment over time in the Sunan economic region. The results are similar to the spatiotemporal trajectories that we observe among some Western European countries (Gellrich et al., 2007; Levers et al., 2018; Rigg et al., 2018), which may extend the application of the Ricardian comparative advantage and Alonso's bid rent theory. Farmland abandonment was the answer to the decreasing trend in the profitability of agriculture (Gellrich et al., 2007). Specifically, the rising opportunity costs in traditional farming may encourage farmers to prioritize off-farm jobs over farming activities, thus predisposing some fields to be abandoned or transformed into built-up areas. Similarly, with rapid socio-economic development, the income gap between agricultural and non-agricultural sectors gradually widens (Xu et al., 2019), and farmers may not generate satisfying economic returns. As a consequence, the decreasing comparative advantage forces rural labors to give up traditional farming and engage in off-farm employment in urbanized areas (Lambin and Meyfroidt, 2010; Yan et al., 2016). In turn, this phenomenon aggravates the reduction of agricultural inputs or even the abandonment of farming on productive soils. Such observations may stimulate an intervention by the government to preserve best-endowed cultivated areas around the cities. At the same time, farmers may switch to more profitable crops that are in high demand among urban dwellers. Our regression analysis also evidenced that appropriately transforming cereal crops to the cultivation of cash crops can decrease the likelihood of farmland abandonment. Thus, the Ricardian comparative advantage theory and Alonso's bid rent theory could also be carefully applied in specifying future land-management practices when agricultural fields are favored over time for other agricultural uses.

Speculation behaviors on the rising land value may also result in farmland abandonment in rapidly urbanized areas. Due to ongoing urbanization, the gross returns from agricultural production might be much lower compared with the rising land value. Therefore, farmers might be willing to discontinue their operations and exit farming and instead to engage in off-farm employment to maximize their profits (Gould et al., 2006; Roebeling and Hendrix, 2010). As a vicious circle, such indirect stimulation of rural–urban migration might increase the demands for land to convert into urbanized areas. However, the fluctuated odds ratio of '*Land prices*' in our statistical analysis suggests that the impacts of land prices on farmland abandonment should be interpreted with more cautions because such causal relationship may be time-varying and be affected by the intervention of some other proximate causes, such as contemporary land-management practices. For instance, in Sunan economic region, policies were implemented in 2010

to curb excessive increases in land-leasing prices. Despite the positive outcomes on stabilizing land prices and curbing speculation behaviors, however, such actions may result in low-intensity farming operations and even unintended temporary farmland abandonment to pursue higher profits from off-farm employments in the urban fringe. At the same time, Sunan has undergone faster farmland transfer from one land user to another than other regions in China (Gao et al., 2019; Luo, 2018). Such faster land transfer from inefficient to more efficient land users may reduce unintended farmland abandonment.

The present study provided spatially explicit information regarding farmland abandonment and recultivation at an inter-annual temporal level. However, mapping land abandonment in rapidly urbanized areas may still pose challenges linking to small and highly fragmented plots. In part, we recognized this problem by using an urban built-up mask to eliminate the misclassified plots within inner cities. Furthermore, we also controlled for inter-annual fallow as a part of crop rotation. This measure can better understand the complexity of double cropping but also allow us to identify the small plots undergoing fallow or temporary cultivation. Nevertheless, the improvements in the classification accuracy of land abandonment in heterogeneous and highly fragmented urban settings warrant increasing attention in the future. Phenological metrics deriving from sub-optimal datasets, for instance, can be used to distinguish the spectral differences between abandoned fields and stable farmland as obtained by Grădinaru et al. (2019). Notably, the transferability of the mapping method should account for the availability of no shadow multi-seasonal images as well as the varying phenological calendar of the vegetation in different climatic conditions (Grădinaru et al., 2019). Alternatively, higher resolution images, such as Sentinel-2 images provided by the European Space Agency, can be applied to identify more nuanced trajectories of agricultural land-use associated with farmland abandonment and recultivation. However, it is often restricted by considerable man-power, time-consuming as well as the long-term availability.

Our results have important policy implications on land-use decisions in response to farmland abandonment that evolves from ongoing urbanization and socio-economic transitions. As the likelihood of farmland abandonment increased with distance from the major settlements, farming structures should be spatially adjusted for filling the income gaps between traditional agriculture and non-agricultural sectors to prevent more abandoned fields. Given the higher opportunity costs of rural labor and the greater comparative advantages of market accessibility, areas close to urbanized areas should cultivate products that have greater ratios of advantage. More specifically, some agricultural commodities with a higher market value could be prioritized to be cultivated near cities, while cereal crops could be appropriately adjusted to places a little farther away from urbanized areas. From this standpoint, Ricardian comparative advantage theory and Alonso's bid rent theory may provide theoretical guidance for optimizing farming structures along the rural–urban gradient to economically maximize outputs. Furthermore, to satisfy the escalating demands for food self-reliance at a broader scale, some incentive policies for the cereal production system may be effective strategies to intensify the existing outputs and explore idle agricultural potentials.

The idle agricultural potential of abandoned farmland provides opportunities to not only fill the income gaps between agricultural production and non-agricultural sectors but also ensure food supply at a broader scale. With increasing urbanization worldwide, we estimate that there might be more farmland abandonment in the coming era. Therefore, we suggest that the spatially shaping role of urbanization in agricultural land-use changes should be given more attention in future land-use planning to avoid unwanted environmental and societal outcomes.

## 5. Conclusion

Despite efforts to explore the patterns and drivers of farmland abandonment worldwide, we know very little about how the urbanization that accompanies socio-economic transitions shapes agricultural land-use in space and time, which hinders the implementation of regionalized and targeted policies to avoid unwanted outcomes. To our knowledge, the present study is the first attempt in China to move away from temporal land-change intervals and employ Landsat imageries to reconstruct farmland abandonment with detailed time-series. Our analysis demonstrates that the Sunan economic region of China has undergone a drastic transformation from an agricultural-dominated landscape to a highly urbanized landscape since the 21st century, and widespread farmland abandonment was identified, although recultivation or conversion to other land uses occurred quickly. Methodologically, our classification accuracies confirm the suitability of our approach of applying the Classification and Regression Trees (CART) classifier in GEE to map farmland abandonment and recultivation with detailed time-series based on 30-m-resolution Landsat imageries. The separate classification for the two annual growing seasons of the same year can minimize the impacts of the fuzzy spectral signature and the complexity of double cropping while controlling for inter-annual fallow as a part of crop rotation. Moreover, we identified the determinants of farmland abandonment for each period using spatially explicit logistic regression models at the pixel level. The results suggest that locational characteristics and socio-economic transitions played key roles in shaping agricultural land-use in space and time. Such insights can provide some guidance to predict abandonment patterns in response to ongoing urbanization in the future. Theoretically, although the spatial causality coincided with Von Thünen's model, which states that the agricultural pattern and intensity are determined by the locational characteristics to some extent, we are convinced that the causal chain that underlies how urban expansion spatially determines farmland

abandonment is more suitably explained using Ricardian comparative advantage theory and Alonso's bid rent theory because of the decreasing trend in the profitability of agriculture compared to non-agricultural sectors. Given the strong socio-economic and environmental effects of massive farmland abandonment, the shaping role of urbanization in agricultural land-use changes must be given more attention in future policy-making because efficient utilization of abandoned fields will not only acquire reasonable environmental returns but also satisfy the escalating demands for agricultural commodities.

### CRediT authorship contribution statement

**Dawei Hou:** Conceptualization, Methodology, Software, Formal analysis, Writing - original draft. **Fanhao Meng:** Data curation, Software, Funding acquisition. **Alexander V. Prishchepov:** Supervision, Writing - review & editing, Funding acquisition.

### Acknowledgments

We sincerely thanks for the constructive comments from Prof. Daniel Müller (IAMO) and Tzu-Hsin Karen Chen (Yale University). We acknowledge funding of the DFF-Danish ERC Support Program (grant number: 116491, 9127-00001B), the Overseas Expertise Introduction Project for Discipline Innovation (111 Project) (Grant No. B17024), Research Fund Program of Guangdong Provincial Key Laboratory of Environmental Pollution Control and Remediation Technology (Grant No. 2018K01) and Scientific Research Start-up Fund Projects of Introduced Talents (Grant No. 5909001803).

### Appendix A

**Table A1**  
Training data for each growing season.

	FA	FORE	IM	OL	WA	Total		FA	FORE	IM	OL	WA	Total
2001I	981	262	500	295	146	2184	2001II	988	173	419	175	135	1890
2002I	831	178	438	190	156	1793	2002II	851	155	379	226	118	1729
2003I	731	182	420	225	134	1692	2003II	825	175	463	162	128	1753
2004I	830	148	378	232	116	1704	2004II	587	145	359	183	131	1405
2005I	665	133	400	197	130	1525	2005II	680	128	404	184	137	1533
2006I	779	167	417	183	151	1697	2006II	825	152	360	192	145	1674
2007I	816	143	414	151	156	1680	2007II	891	158	390	173	135	1747
2008I	630	165	334	169	140	1438	2008II	622	116	341	194	141	1414
2009I	733	126	355	190	107	1511	2009II	650	168	342	184	112	1456
2010I	438	125	297	160	116	1136	2010II	577	152	340	159	144	1372
2011I	530	126	347	179	113	1295	2011II	474	183	371	182	107	1317
2012I	896	117	335	172	115	1635	2012II	438	134	260	166	135	1133
2013I	849	158	256	167	129	1559	2013II	723	145	257	185	119	1429
2014I	365	147	245	186	154	1097	2014II	354	134	280	197	110	1075
2015I	473	153	281	151	111	1169	2015II	754	118	253	157	107	1389
2016I	530	158	342	184	108	1322	2016II	416	158	326	160	104	1164
2017I	389	110	305	173	145	1122	2017II	450	188	269	170	105	1182
2018I	722	175	274	140	124	1435	2018II	432	121	215	156	155	1079

Note: 'I' represented Spring-growing season in each year; 'II' represented Fall-growing season in each year. Abbreviation for land cover types: FA-'Farmland'; FORE-'Forest'; IM-'Impervious surface'; OL-'Other' and WA-'Water'.

**Table A2**  
Training data for each growing season.

	FA	FORE	IM	OL	WA	Total		FA	FORE	IM	OL	WA	Total
2001I	386	128	230	109	79	932	2001II	348	105	203	95	77	828
2002I	333	111	198	88	81	811	2002II	320	101	176	105	74	776
2003I	308	111	184	95	77	775	2003II	315	105	206	92	76	794
2004I	331	105	176	96	73	781	2004II	267	99	184	97	77	724

(continued on next page)

**Table A2 (continued)**

	FA	FORE	IM	OL	WA	Total		FA	FORE	IM	OL	WA	Total
2005I	298	102	210	89	76	775	2005II	286	96	181	97	78	738
2006I	324	109	203	87	80	803	2006II	315	100	172	98	79	764
2007I	313	104	183	80	81	761	2007II	328	102	178	95	77	780
2008I	276	108	167	84	78	713	2008II	274	93	189	99	78	733
2009I	296	100	171	88	71	726	2009II	280	104	181	97	72	734
2010I	264	100	180	82	73	699	2010II	265	100	168	92	79	704
2011I	279	100	195	86	73	733	2011II	245	107	174	96	71	693
2012I	329	99	168	84	73	753	2012II	238	97	172	93	77	677
2013I	320	107	155	83	76	741	2013II	295	99	193	97	74	758
2014I	228	105	169	87	81	670	2014II	221	97	196	99	72	685
2015I	246	106	176	80	72	680	2015II	301	94	151	91	71	708
2016I	288	107	186	87	72	740	2016II	233	102	165	92	71	663
2017I	249	97	186	85	79	696	2017II	240	108	154	94	71	667
2018I	301	110	175	78	75	739	2018II	236	94	183	91	81	685

Note: 'I' represented Spring-growing season in each year; 'II' represented Fall-growing season in each year. Abbreviation for land cover types: FA-'Farmland'; FORE-'Forest'; IM-'Impervious surface'; OL-'Other' and WA-'Water'.

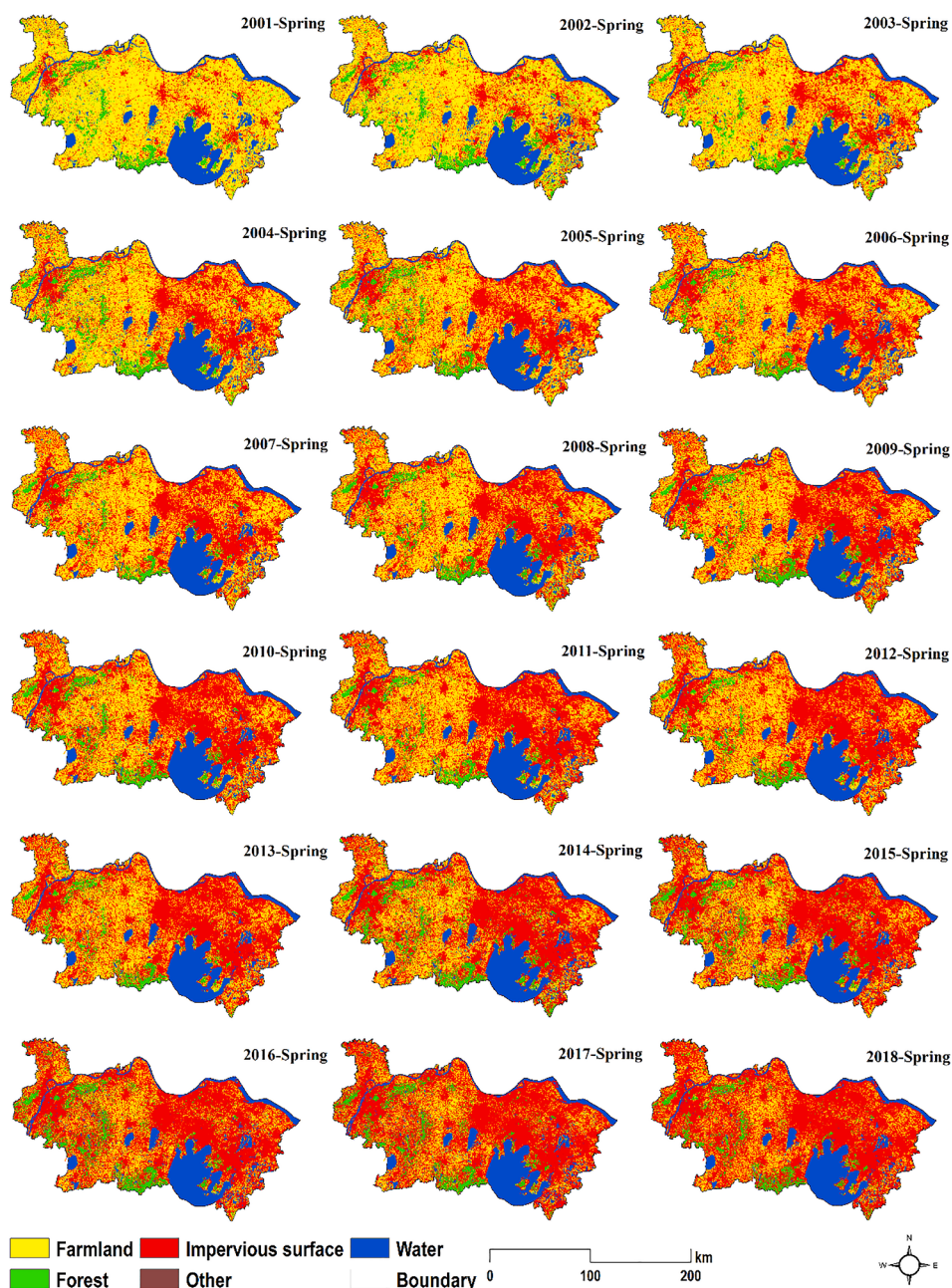
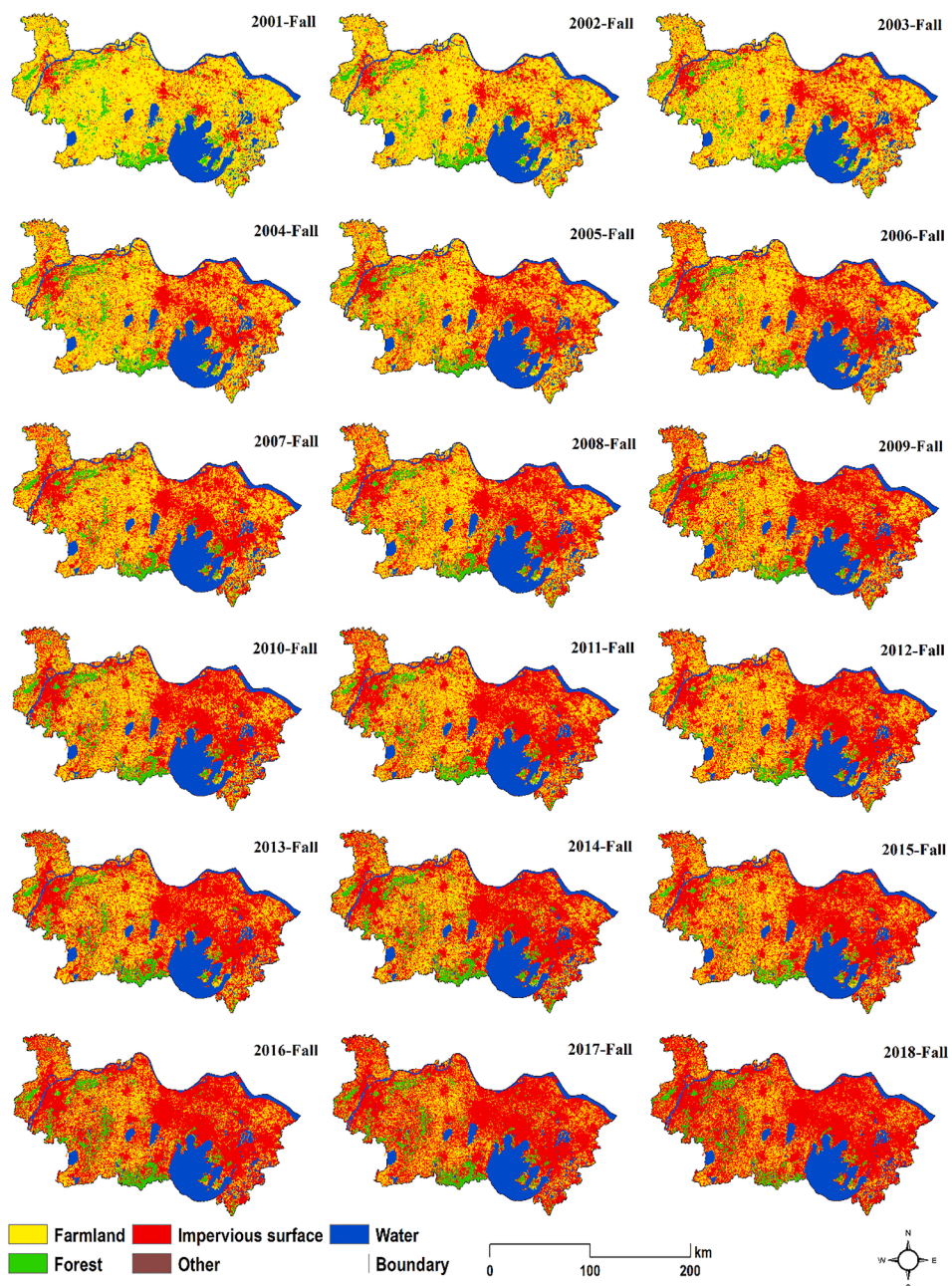


Fig. A3. Land use/cover classification in all 18 Spring-growing seasons from 2001 to 2018.



**Fig. A4.** Land use/cover classification in all 18 Fall-growing seasons from 2001 to 2018.

**Table A5**

The summary of confusion matrix in all 36 growing seasons from 2001 to 2018.

	FA	FORE	IM	OL	WA	PA (Fall)	UA (Fall)	OA
FA	8959	131	301	75	89	93.71( $\pm 4.45$ )	92.62( $\pm 3.27$ )	
FORE	133	1940	3	1	0	92.79( $\pm 5.69$ )	92.48( $\pm 7.52$ )	
IM	375	1	4400	185	1	89.3( $\pm 5.15$ )	91.03( $\pm 7.41$ )	
OL	92	0	163	2356	2	91.51( $\pm 6.95$ )	91( $\pm 6.19$ )	
WA	75	5	6	9	1713	95.57( $\pm 2.74$ )	92.46( $\pm 7.55$ )	
PA(Spring)	94.95( $\pm 2.97$ )	93.75( $\pm 6.25$ )	89.24( $\pm 6.03$ )	90( $\pm 7.38$ )	93.57( $\pm 4.68$ )			
UA(Spring)	93.63( $\pm 3.5$ )	91.8( $\pm 7.32$ )	91.36( $\pm 4.2$ )	89.32( $\pm 5.76$ )	95.12( $\pm 4.88$ )			
OA								92.84( $\pm 2.58$ )

Abbreviation: FA—‘Farmland’; FORE—‘Forest’; IM—‘Impervious surface’; OL—‘Other’; WA—‘Water’; PA (Fall)—‘Producer’s accuracy in Fall-growing seasons’; PA (Spring)—‘Producer’s accuracy in Spring-growing seasons’; UA (Spring)—‘User’s accuracy in Spring-growing seasons’; UA (Fall)—‘User’s accuracy in Fall-growing seasons’ and OA—‘Overall accuracy’.

## Appendix B. Supplementary data

Supplementary data to this article can be found online at <https://doi.org/10.1016/j.landurbplan.2021.104170>.

## References

- Achieng, T., Maciejewski, K., Dyer, M., & Biggs, R. (2020). Using a social-ecological regime shift approach to understand the transition from livestock to game farming in the Eastern Cape, South Africa. *Land*, 9, 97.
- Arnaez, J., Lasanta, T., Errea, M. P., & Ortigosa, L. (2011). Land abandonment, landscape evolution, and soil erosion in a Spanish Mediterranean mountain region: The case of Camero Viejo. *Land Degradation and Development*, 22, 537–550.
- Barlowe, R. (1986). *Land Resource Economics: The Economics of Real Estate* (4th ed.). Englewood Cliffs NJ: Prentice-Hall.
- Baumann, M., Kuemmerle, T., Elbakidze, M., Ozdogan, M., Radeloff, V. C., Keuler, N. S., ... Hostert, P. (2011). Patterns and drivers of post-socialist farmland abandonment in Western Ukraine. *Land Use Policy*, 28, 552–562.
- Bürgi, M., Hersperger, A. M., & Schneeberger, N. (2004). Driving forces of landscape change – current and new directions. *Landscape Ecology*, 19, 857–868.
- Bren D'Amour, C., Reitsma, F., Baochchi, G., Barthel, S., Güneralp, B., Erb, K., Creutzig, ... Seto, K. C. (2017). Future urban land expansion and implications for global croplands. *Proceedings of the National Academy of Sciences*, 114, 8939–8944.
- Chaudhary, S., Wang, Y., Dixit, A. M., Khanal, N. R., Xu, P., Fu, B., ... Li, M. (2020). A Synopsis of farmland abandonment and its driving factors in Nepal. *Land*, 9, 84.
- Dara, A., Baumann, M., Freitag, M., Hözel, N., Hostert, P., Kamp, J., ... Kuemmerle, T. (2020). Annual Landsat time series reveal post-Soviet changes in grazing pressure. *Remote Sensing of Environment*, 239, Article 111667.
- Dara, A., Baumann, M., Kuemmerle, T., Pflugmacher, D., Rabe, A., Griffiths, P., ... Hostert, P. (2018). Mapping the timing of cropland abandonment and recultivation in northern Kazakhstan using annual Landsat time series. *Remote Sensing of Environment*, 213, 49–60.
- Deng, X., Huang, J., Rozelle, S., Zhang, J., & Li, Z. (2015). Impact of urbanization on cultivated land changes in China. *Land Use Policy*, 45, 1–7.
- Díaz, G. I., Nahuelhual, L., Echeverría, C., & Marín, S. (2011). Drivers of land abandonment in Southern Chile and implications for landscape planning. *Landscape Urban Plan*, 99, 207–217.
- Dubinin, M., Potapov, P., Lushchekina, A., & Radeloff, V. C. (2010). Reconstructing long time series of burned areas in arid grasslands of southern Russia by satellite remote sensing. *Remote Sensing of Environment*, 114, 1638–1648.
- Elbakidze, M., & Angelstam, P. (2007). Implementing sustainable forest management in Ukraine's Carpathian Mountains: The role of traditional village systems. *Forest Ecology and Management*, 249, 28–38.
- Ellison, C. E., & Bachrach, D. (2013). Dosage compensation via transposable element mediated rewiring of a regulatory network. *Science*, 342, 846–850.
- FAO. (2006). *The role of agriculture and rural development in revitalizing abandoned/depopulated areas*. Food and Agriculture Organization of the United Nations.
- Gao, L., Sun, D., & Ma, C. (2019). The Impact of Farmland Transfers on Agricultural Investment in China: A Perspective of Transaction Cost Economics. *China & World Economy*, 27, 93–109.
- Gellrich, M., Baur, P., Koch, B., & Zimmermann, N. E. (2007). Agricultural land abandonment and natural forest re-growth in the Swiss mountains: A spatially explicit economic analysis. *Agriculture, Ecosystems & Environment*, 118, 93–108.
- Ge, D., Long, H., Zhang, Y., Ma, L., & Li, T. (2018). Farmland transition and its influences on grain production in China. *Land Use Policy*, 70, 94–105.
- Gould, K. A., Carter, D. R., & Shrestha, R. K. (2006). Extra-legal land market dynamics on a Guatemalan agricultural frontier: Implications for neoliberal land policies. *Land Use Policy*, 23, 408–420.
- Gilabert, M. A., González-Piqueras, J., García-Haro, F. J., & Meliá, J. (2002). A generalized soil-adjusted vegetation index. *Remote Sensing of Environment*, 82, 303–310.
- Gorelick, N., Hancher, M., Dixon, M., Ilyushchenko, S., Thau, D., & Moore, R. (2017). Google Earth Engine: Planetary-scale geospatial analysis for everyone. *Remote Sensing of Environment*, 202, 18–27.
- Grădinariu, S. R., Kienast, F., & Psomas, A. (2019). Using multi-seasonal Landsat imagery for rapid identification of abandoned land in areas affected by urban sprawl. *Ecological Indicators*, 96, 79–86.
- Grădinariu, S. R., Iojă, C. I., Onose, D. A., Gavrilidis, A. A., Pătru-Stupariu, I., Kienast, F., & Hersperger, A. M. (2015). Land abandonment as a precursor of built-up development at the sprawling periphery of former socialist cities. *Ecological Indicators*, 57, 305–313.
- Han, Z., & Song, W. (2019). Spatiotemporal variations in cropland abandonment in the Guizhou-Guangxi karst mountain area, China. *Journal of Cleaner Production*, 238, Article 117888.
- He, C., Liu, Z., Xu, M., Ma, Q., & Dou, Y. (2017). Urban expansion brought stress to food security in China: Evidence from decreased farmland net primary productivity. *Science of the Total Environment*, 576, 660–670.
- Hosmer, D. W., & Lemeshow, S. (2000). *Applied logistic regression* (2nd ed.). New York: Wiley & Sons.
- Höchtl, F., Lehringer, S., & Konold, W. (2005). "Wilderness": What it means when it becomes a reality—A case study from the southwestern Alps. *Landscape Urban Plan*, 70, 85–95.
- Huang, H., Chen, Y., Clinton, N., Wang, J., Wang, X., Liu, C., ... Zhu, Z. (2017). Mapping major land cover dynamics in Beijing using all Landsat images in Google Earth Engine. *Remote Sensing of Environment*, 202, 166–176.
- Huber, P. J. (1967). The behavior of maximum likelihood estimates under nonstandard conditions. In *Proceedings of the Fifth Berkeley Symposium on Mathematical Statistics and Probability*, Berkeley, CA, USA (pp. 221–233).
- Jackson, T. (2004). Vegetation water content mapping using Landsat data derived normalized difference water index for corn and soybeans. *Remote Sensing of Environment*, 92, 475–482.
- Johansen, K., Phinn, S., & Taylor, M. (2015). Mapping woody vegetation clearing in Queensland, Australia from Landsat imagery using the Google Earth Engine. *Remote Sensing Applications: Society and Environment*, 1, 36–49.
- Kroll, F., Müller, F., Haase, D., & Fohrer, N. (2012). Rural–urban gradient analysis of ecosystem services supply and demand dynamics. *Land Use Policy*, 29, 521–535.
- Kuemmerle, T., Hostert, P., Radeloff, V. C., van der Linden, S., Perzanowski, K., & Kruhlav, I. (2008). Cross-border comparison of post-socialist farmland abandonment in the Carpathians. *Ecosystems*, 11, 614–628.
- Lambin, E. F., & Meyfroidt, P. (2010). Land use transitions: Socio-ecological feedback versus socio-economic change. *Land Use Policy*, 27, 108–118.
- Larondelle, N., & Haase, D. (2013). Urban ecosystem services assessment along a rural–urban gradient: A cross-analysis of European cities. *Ecological Indicators*, 29, 179–190.
- Levers, C., Schneider, M., Prishchepov, A. V., Estel, S., & Kuemmerle, T. (2018). Spatial variation in determinants of agricultural land abandonment in Europe. *Science of the Total Environment*, 644, 95–111.
- Lieskovský, J., Bezák, P., Špulová, J., Lieskovský, T., Koleda, P., Dobrovodská, M., ... Gimmi, U. (2015). The abandonment of traditional agricultural landscape in Slovakia – Analysis of extent and driving forces. *Journal of Rural Studies*, 37, 75–84.
- Li, X., Gong, P., & Liang, L. (2015). A 30-year (1984–2013) record of annual urban dynamics of Beijing City derived from Landsat data. *Remote Sensing of Environment*, 166, 78–90.
- Li, Y., Wu, W., & Liu, Y. (2018). Land consolidation for rural sustainability in China: Practical reflections and policy implications. *Land Use Policy*, 74, 137–141.
- Liu, Y., Li, J., & Yang, Y. (2018). Strategic adjustment of land use policy under the economic transformation. *Land Use Policy*, 74, 5–14.
- Liu, M., Han, G., & Zhang, Q. (2020). Effects of agricultural abandonment on soil aggregation, soil organic carbon storage and stabilization: Results from observation in a small karst catchment, Southwest China. *Agriculture, Ecosystems & Environment*, 288, Article 106719.
- Lozano, F. J., Suárez-Seoane, S., Kelly, M., & Luis, E. (2008). A multi-scale approach for modeling fire occurrence probability using satellite data and classification trees: A case study in a mountainous Mediterranean region. *Remote Sensing of Environment*, 112, 708–719.
- Luo, B. (2018). 40-year reform of farmland institution in China: Target, effort and the future. *China Agricultural Economic Review*, 10, 16–35.
- Löw, F., Prishchepov, A., Waldner, F., Dubovik, O., Akramkhanov, A., Biradar, C., & Lamers, J. (2018). Mapping Cropland Abandonment in the Aral Sea Basin with MODIS Time Series. *Remote Sensing-Basel*, 10, 159.
- Meyfroidt, P., Schierhorn, F., Prishchepov, A. V., Müller, D., & Kuemmerle, T. (2016). Drivers, constraints and trade-offs associated with recultivating abandoned cropland in Russia, Ukraine and Kazakhstan. *Global Environmental Change*, 37, 1–15.
- Milenov, P., Vassilev, V., Vassileva, A., Radkov, R., Samoungi, V., Dimitrov, Z., & Vichev, N. (2014). Monitoring of the risk of farmland abandonment as an efficient tool to assess the environmental and socio-economic impact of the Common Agriculture Policy. *International Journal of Applied Earth Observation*, 32, 218–227.
- Munroe, D. K., van Berkela, D. B., Verburg, P. H., & Olson, J. L. (2013). Alternative trajectories of land abandonment: causes, consequences and research challenges. *Current Opinion in Environmental Sustainability*.
- Müller, D., & Munroe, D. K. (2008). Changing rural landscapes in Albania: Cropland abandonment and forest clearing in the postsocialist transition. *Annals of the Association of American Geographers*, 98, 855–876.
- Müller, D., Sun, Z., Vongvisouk, T., Pflugmacher, D., Xu, J., & Mertz, O. (2014). Regime shifts limit the predictability of land-system change. *Global Environmental Change*, 28, 75–83.
- Patel, N. N., Angiuli, E., Gamba, P., Gaughan, A., Lisini, G., Stevens, F. R., ... Trianni, G. (2015). Multi-temporal settlement and population mapping from Landsat using Google Earth Engine. *International Journal of Applied Earth Observation*, 35, 199–208.
- Prishchepov, A. V., Schierhorn, F., & Löw, F. (2021). Unraveling the diversity of trajectories and drivers of global agricultural land abandonment. *Land*, 10, 97.
- Prishchepov, Alexander V. (2020). Agricultural Land Abandonment. *Environmental Science*, by Alexander V. Prishchepov. Oxford University Press.
- Prishchepov, A. V., Müller, D., Dubinin, M., Baumann, M., & Radeloff, V. C. (2013). Determinants of agricultural land abandonment in post-Soviet European Russia. *Land Use POLICY*, 30, 873–884.
- Prishchepov, A. V., Radeloff, V. C., Baumann, M., Kuemmerle, T., & Müller, D. (2012). Effects of institutional changes on land use: Agricultural land abandonment during the transition from state-command to market-driven economies in post-Soviet Eastern Europe. *Environmental Research Letters*, 7, 24021.
- Qiu, B., Yang, X., Tang, Z., Chen, C., Li, H., & Berry, J. (2020). Urban expansion or poor productivity: Explaining regional differences in cropland abandonment in China during the early 21st century. *Land Degradation & Development*.
- Renwick, A., Jansson, T., Verburg, P. H., Revoredo-Giha, C., Britz, W., Gocht, A., & McCracken, D. (2013). Policy reform and agricultural land abandonment in the EU. *Land Use Policy*, 30, 446–457.

- Roebeling, P. C., & Hendrix, E. M. T. (2010). Land speculation and interest rate subsidies as a cause of deforestation: The role of cattle ranching in Costa Rica. *Land Use Policy*, 27, 489–496.
- Rigg, J., Salamanca, A., Phongsiri, M., & Sripun, M. (2018). More farmers, less farming? Understanding the truncated agrarian transition in Thailand. *World Development*, 107, 327–337.
- Schierhorn, F., Kastner, T., Kuemmerle, T., Meyfroidt, P., Kurganova, I., Prishchepov, A. V., ... Müller, D. (2019). Large greenhouse gas savings due to changes in the post-Soviet food systems. *Environmental Research Letters*, 14, 65009.
- Seto, K. C., & Ramankutty, N. (2016). Hidden linkages between urbanization and food systems. *Science*, 352, 943–945.
- Seto, K. C., & Kaufmann, R. K. (2003). Modeling the drivers of urban land use change in the Pearl River Delta, China: Integrating remote sensing with socioeconomic data. *Land Economy*, 79, 106–121.
- Seto, K. C., Reenberg, A., Boone, C. G., Fragkias, M., Haase, D., Langanke, T., ... Simon, D. (2012). Urban land teleconnections and sustainability. *Proceedings of the National Academy of Sciences*, 109, 7687–7692.
- Shi, T., Li, X., Xin, L., & Xu, X. (2018). The spatial distribution of farmland abandonment and its influential factors at the township level: A case study in the mountainous area of China. *Land Use Policy*, 70, 510–520.
- Sileika, A. S., Stalnacke, P., Kutra, S., Gaigalis, K., & Berankiene, L. (2006). Temporal and Spatial Variation of Nutrient Levels in the Nemunas River (Lithuania and Belarus). *Environmental Monitoring and Assessment*, 122, 335–354.
- Tsutsumida, N., & Comber, A. J. (2015). Measures of spatio-temporal accuracy for time series land cover data. *International Journal of Applied Earth Observation*, 41, 46–55.
- van der Zanden, E. H., Verburg, P. H., Schulp, C. J. E., & Verkerk, P. J. (2017). Trade-offs of European agricultural abandonment. *Land Use Policy*, 62, 290–301.
- Verburg, P. H., & Overmars, K. P. (2009). Combining top-down and bottom-up dynamics in land use modeling: Exploring the future of abandoned farmlands in Europe with the Dyna-CLUE model. *Landscape Ecology*, 24, 1167–1181.
- Vinogradovs, I., Nikodemus, O., Elferts, D., & Brümelis, G. (2018). Assessment of site-specific drivers of farmland abandonment in mosaic-type landscapes: A case study in Vidzeme, Latvia. *Agriculture, Ecosystems & Environment*, 253, 113–121.
- Weisseiner, C. J., Boschetti, M., Böttcher, K., Carrara, P., Bordogna, G., & Brivio, P. A. (2011). Spatial explicit assessment of rural land abandonment in the Mediterranean area. *Global and Planetary Change*, 79, 20–36.
- White, H. (1982). Maximum likelihood estimation of misspecified models. *Econometrica*, 50, 1–25.
- Wang, Y., Li, X., Xin, L., & Tan, M. (2020). Farmland marginalization and its drivers in mountainous areas of China. *Science of the Total Environment*, 719, Article 135132.
- Wright, C., & Gallant, A. (2007). Improved wetland remote sensing in Yellowstone National Park using classification trees to combine TM imagery and ancillary environmental data. *Remote Sensing of Environment*, 107, 582–605.
- Xie, Y., Batty, M., & Zhao, K. (2007). Simulating emergent urban form using agent-based modeling: Desakota in the Suzhou-Wuxian Region in China. *Annals of the Association of American Geographers*, 97, 477–495.
- Xu, D., Deng, X., Guo, S., & Liu, S. (2019). Labor migration and farmland abandonment in rural China: Empirical results and policy implications. *Journal of Environment Management*, 232, 738–750.
- Xu, M., Watanachaturaporn, P., Varshney, P., & Arora, M. (2005). Decision tree regression for soft classification of remote sensing data. *Remote Sensing of Environment*, 97, 322–336.
- Yan, J., Yang, Z., Li, Z., Li, X., Xin, L., & Sun, L. (2016). Drivers of cropland abandonment in mountainous areas: A household decision model on farming scale in Southwest China. *Land Use Policy*, 57, 459–469.
- Yin, H., Brandão, A., Buchner, J., Helmers, D., Iuliano, B. G., Kimambo, N. E., ... Radeloff, V. C. (2020). Monitoring cropland abandonment with Landsat time series. *Remote Sensing of Environment*, 246, Article 111873.
- Yin, H., Butsic, V., Buchner, J., Kuemmerle, T., Prishchepov, A. V., Baumann, M., ... Radeloff, V. C. (2019). Agricultural abandonment and re-cultivation during and after the Chechen Wars in the northern Caucasus. *Global Environmental Change*, 55, 149–159.
- Yin, H., Prishchepov, A. V., Kuemmerle, T., Bleyhl, B., Buchner, J., & Radeloff, V. C. (2018). Mapping agricultural land abandonment from spatial and temporal segmentation of Landsat time series. *Remote Sensing of Environment*, 210, 12–24.
- Zabel, F., Putzenlechner, B., & Mauser, W. (2014). Global agricultural land resources—a high resolution suitability evaluation and its perspectives until 2100 under climate change conditions. *PLoS ONE*, 9, Article e107522.
- Zhang, Y., Li, X., & Song, W. (2014). Determinants of cropland abandonment at the parcel, household and village levels in mountain areas of China: A multi-level analysis. *Land Use Policy*, 41, 186–192.
- Zhou, T., Koomen, E., & Ke, X. (2020). Determinants of farmland abandonment on the urban-rural fringe. *Environmental Management*, 65, 369–384.
- Zurqani, H. A., Post, C. J., Mikhailova, E. A., Schlautman, M. A., & Sharp, J. L. (2018). Geospatial analysis of land use change in the Savannah River Basin using Google Earth Engine. *International Journal of Applied Earth Observation*, 69, 175–185.
- Zhu, Z., & Woodcock, C. E. (2012). Object-based cloud and cloud shadow detection in Landsat imagery. *Remote Sensing of Environment*, 118, 83–94.